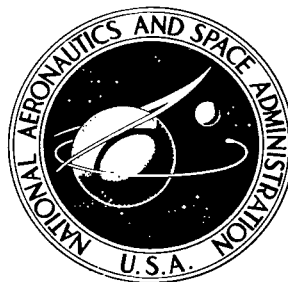


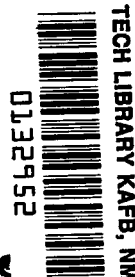
NASA TECHNICAL NOTE



NASA TN D-6428

e.1

NASA TN D-6428



TECH LIBRARY KAFB, NM

**LOAN COPY: RETURN TO
AFWL (DOGL)
KIRTLAND AFB, N. M.**

IN-FLIGHT USE OF TRAVERSING BOUNDARY-LAYER PROBES

by Edwin J. Saltzman

Flight Research Center

Edwards, Calif. 93523



0132952

1. Report No.	2. Government Accession No.	3. Recipient's Catalog No.	
NASA TN D-6428		5. Report Date July 1971	
4. Title and Subtitle IN-FLIGHT USE OF TRAVERSING BOUNDARY-LAYER PROBES		6. Performing Organization Code	
7. Author(s) Edwin J. Saltzman		8. Performing Organization Report No. H-640	
9. Performing Organization Name and Address NASA Flight Research Center P. O. Box 273 Edwards, California 93523		10. Work Unit No. 126-13-02-02-24	
12. Sponsoring Agency Name and Address National Aeronautics and Space Administration Washington, D. C. 20546		11. Contract or Grant No.	
15. Supplementary Notes		13. Type of Report and Period Covered Technical Note	
16. Abstract Two prototype traversing boundary-layer pitot probes were demonstrated in flight. A motor-operated screw-driven type of probe was used on two jet aircraft for defining boundary layers at profile edge Mach numbers from 0.5 to 2.2. The other type of traversing probe was motor driven through a Scotch yoke mechanism and was operated on several flights of the X-15 airplane. The highest free-stream Mach number reached during this series of flights was 5.6. The mechanical and electrical features of these probes are described, and photographs and conceptual drawings are included. Problems encountered during the development of the devices are described, and the solutions that were found are explained. Boundary-layer profile data are presented in several forms, and local friction coefficients derived from the profile through a Clauser type of determination are shown.		14. Sponsoring Agency Code	
17. Key Words (Suggested by Author(s)) In-flight boundary-layer-measurement techniques	18. Distribution Statement Unclassified - Unlimited		
19. Security Classif. (of this report) Unclassified	20. Security Classif. (of this page) Unclassified	21. No. of Pages 32	22. Price* \$3.00

IN-FLIGHT USE OF TRAVERSING BOUNDARY-LAYER PROBES

Edwin J. Saltzman
Flight Research Center

INTRODUCTION

Velocity profiles representing the viscous boundary layer next to the inside wall of a pipe or wind tunnel or the outside skin of an aircraft have been obtained with fixed boundary-layer rakes or a cluster of probes, called a mouse, for many years (refs. 1 to 4). Such devices have provided most of the existing boundary-layer data; however, for certain applications the rake or mouse has disadvantages. One objection to closely spaced probes is their possible mutual interference, especially for laminar boundary layers or turbulent layers at low speeds. Another problem may result from the large number of individual sensors or transducers and recording channels required if a commutating type of valve-sensor, such as was used in reference 4, is not available.

The wind-tunnel boundary-layer practitioners avoided these problems, even during the early days of aerodynamic experimenting, by using traversing devices. These devices made it possible for a single probe or a gang of widely spaced probes to survey the entire boundary layer. Reference 2 and references 5 to 16 are examples of studies in which traversing devices were used in wind-tunnels.

In-flight boundary-layer measurements represent a small part of experimental boundary-layer history. Thus, it is not surprising that the development of the traversing probe concept in flight has been retarded. References 17 and 18 describe early applications of intermittently movable probes for defining the wake profile behind an airfoil in flight. A more recent continuously moving probe for a similar use on gliders is discussed in reference 19.

It became apparent that traversing devices would greatly improve the capability of defining high-speed in-flight boundary layers if they could be made compact and flight worthy. Thus, the Flight Research Center began the development of two types of traversing mechanisms in 1962. This paper presents developmental results from these two types of continuously moving probes. These probes, one driven by a reversible motor and screw and the other through a Scotch yoke, were briefly described in reference 20 and are considered to be prototypes. The purpose in reporting these results and describing the devices is, in part, to encourage the use of traversing probes at higher flight speeds than those for which they have been used. In addition, this report is a response to requests for more information than could be included in reference 20.

The traversing probes described herein were used on three different aircraft at the Flight Research Center. Local Mach numbers ranged up to 2.2 at the boundary-layer edge. One of the devices probed the bottom portion of the boundary layer where peak total temperatures near 1675° K (3020° R), resulting from a free-stream Mach number of 5.6, were encountered. Schematic drawings, photographs, and

boundary-layer profile data are presented for both types of traversing probes, and a comparison is made with fixed-probe rake results. In addition, distribution profiles for momentum and displacement thickness as well as derived friction coefficients are presented for the screw-driven probe.

SYMBOLS

Physical quantities in this report are given in the International System of Units (SI) and parenthetically in U. S. Customary Units. The measurements were taken in U. S. Customary Units. Factors relating the two systems are presented in reference 21.

C_f	local skin-friction coefficient
M	Mach number
p	static pressure
p_t	stagnation pressure
R	Reynolds number, based on edge conditions, e , and lengths, x , θ , or y
T	absolute temperature
t	time
u	local velocity
u_τ	friction velocity, $\frac{u_e}{\sqrt{\frac{2}{C_f}}}$
x	assumed length of turbulent flow
y	distance from skin
δ	boundary-layer thickness
δ^*	displacement thickness
θ	momentum thickness
μ	absolute viscosity
ρ	density
ν	kinematic viscosity

Subscripts:

e edge conditions

w wall conditions

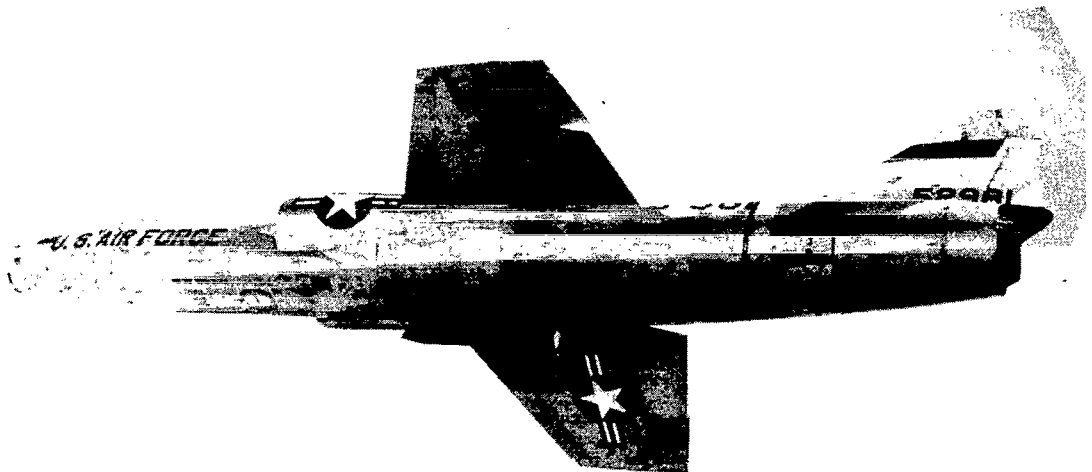
A primed quantity is based on reference temperature conditions of Sommer and Short (ref. 22).

REVERSIBLE SCREW-DRIVEN TRAVERSING PROBES

Airplanes Used and Test Conditions

Two supersonic, turbojet, military type of aircraft, the F-104 and the A5A, were used to obtain turbulent-compressible boundary layers for demonstrating the screw-driven traversing probes.

The F-104 airplane was fitted with an auxiliary ventral fin, which will be referred to as the flight-test fixture. Figure 1(a) is an in-flight photograph of the flight-test-
fixture/aircraft combination. The boundary layer surveyed by the traversing probe was generated on the side of this flight-test fixture, about 121 centimeters (47.6 inches) back from the leading edge or 105.8 centimeters (41.6 inches) aft of the boundary-layer trip.

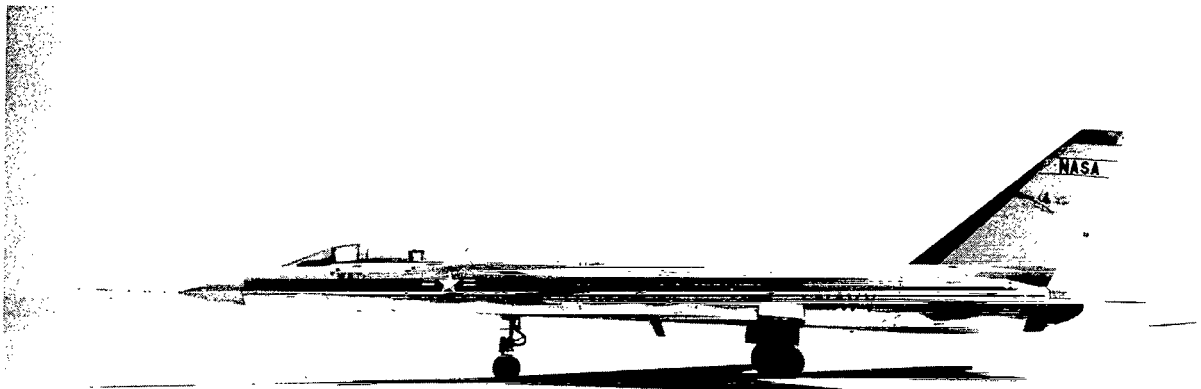


E-18776

(a) F-104 airplane showing flight-test fixture attached to bottom of fuselage.

Figure 1. Test aircraft used to demonstrate screw-driven traversing probe.

Other boundary-layer surveys were made on the bottom surface of the A5A fuselage about 508 centimeters (200 inches) back from the vertex of the fuselage nose. A photograph of the A5A is shown in figure 1(b). The ranges of edge Mach number and



(b) A5A airplane.

E-10548

Figure 1. Concluded.

Reynolds number for the flight tests with these two installations were:

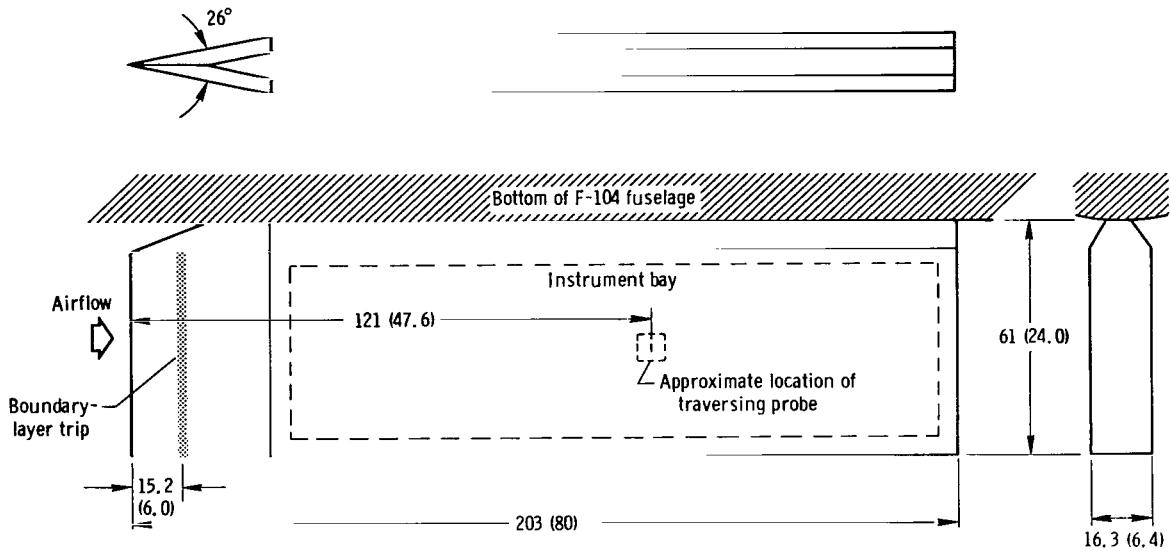
Vehicle	M	R_x	x, cm (in.)
F-104 with flight-test fixture	2.2	1.04×10^7	105.8 (41.6)
A5A	.51 to 1.72	1.54×10^7 to 7.42×10^7	508 (200)

External Installation Details

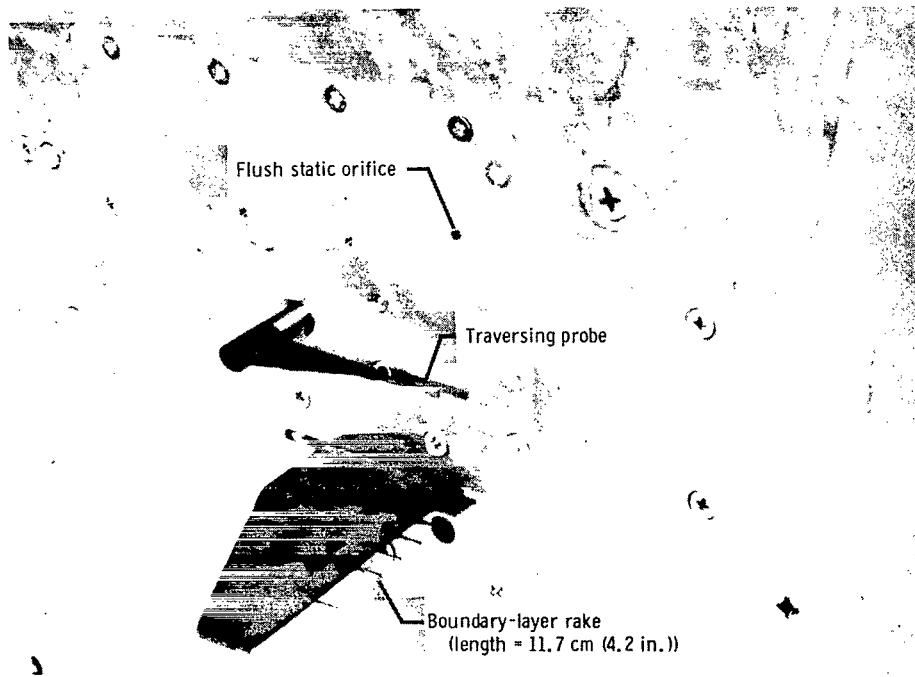
F-104 flight-test fixture. — The flight-test fixture was originally developed as a facility for panel response studies. It contains its own instrumentation, but receives electrical power from the parent aircraft; thus, pressure lines are relatively short and pressure lag values are negligible for most applications. A three-view sketch of the fixture is shown in figure 2(a).

At the probe location the boundary layer was known, through previous experience with the fixture, to be naturally turbulent for the test flight conditions. To insure a nearly fixed length of turbulent run, however, sand-like granules were cemented along a band behind and parallel to the leading edge (fig. 2(a)). The resulting boundary layer was about 16 millimeters to 18 millimeters (0.6 inch to 0.7 inch) thick at the probe station for a local chord station Reynolds number of 1.04×10^7 and a local edge Mach number near 2.2. A photograph of the traversing probe, an accompanying

boundary-layer rake, and flush static orifice is shown in figure 2(b) as they were installed on the side panel of the flight-test fixture.



(a) Three-view sketch. Dimensions in centimeters (inches).



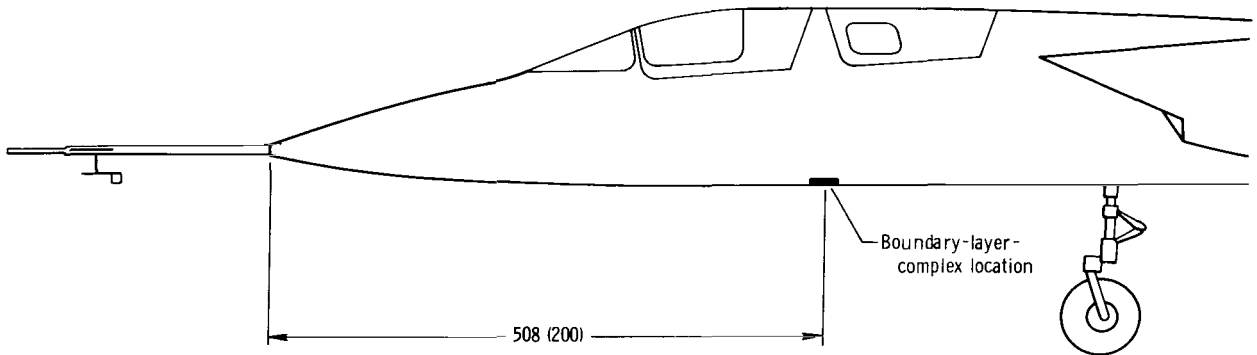
(b) Closeup photo.

E-14512

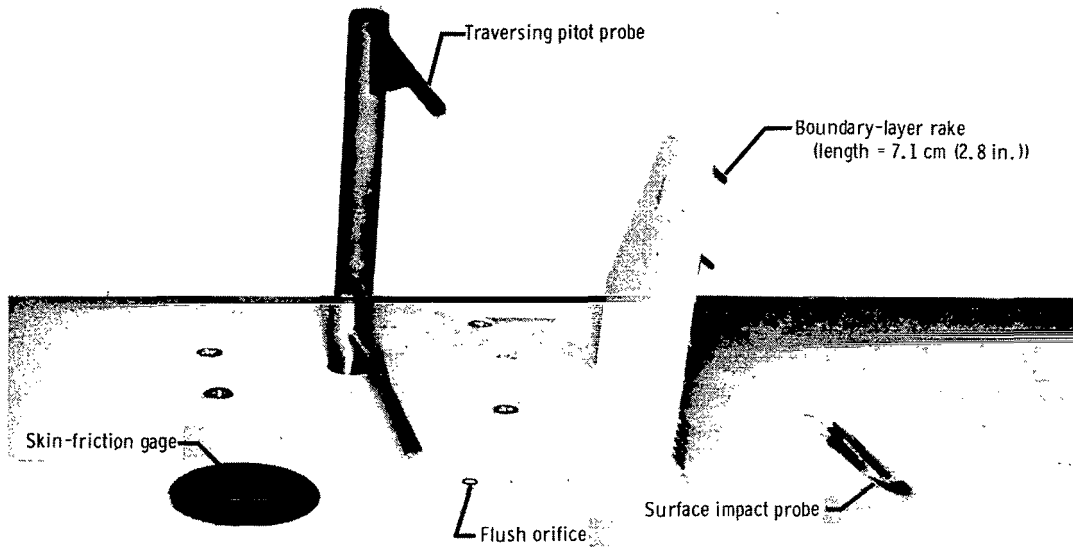
Figure 2. F-104 flight-test-fixture installation.

A5A fuselage. — The lower centerline region of the A5A airplane was chosen as a demonstration site for several devices which were being checked out for flight use. The relative location of this complex of probes and devices is shown in the sketch of figure 3(a). This location was used because the contour was aerodynamically clean and free of gaps or adjacent protuberances. In addition, the 508-centimeter (200-inch) run from the nose assured a turbulent boundary-layer thickness of 5 centimeters to 10 centimeters (2 inches to 4 inches), which is sufficiently thick to be relatively easy to survey. As with the flight-test fixture, the pressure sensors could be placed close to the probes (essentially on the inside of the test surface skin), so that the pressure lines were short enough to avoid lag problems. The local Reynolds numbers based on the assumed length, x , for this installation reached values as high as 7.4×10^7 .

A photograph of the portions of the traversing probe, fixed rake, and other sensors which were exposed to the airstream is shown in figure 3(b). The friction gage did not



(a) Sketch of A5A forebody. Dimensions in centimeters (inches).



(b) Closeup photo.

E-18775

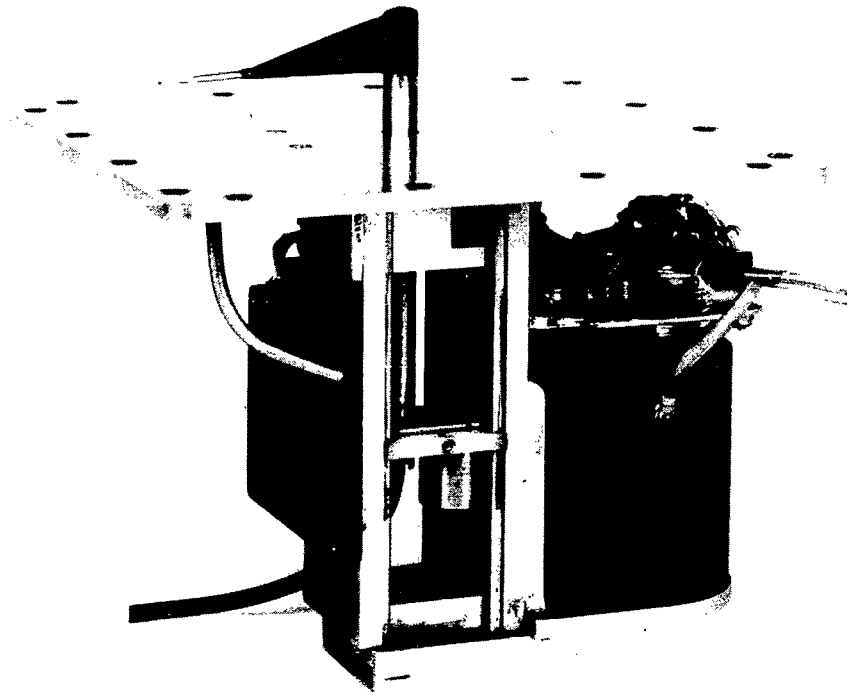
Figure 3. A5A installation.

function properly; thus, comparisons of boundary-layer-derived parameters with direct force measurements cannot be made. For this installation the mast of the traversing probe supported two pitot probes, thus increasing the range of the survey. The A5A installation provided data from a boundary-layer rake and a Preston probe in addition to the traversing probe. Although some data derived from the traversing probe are presented in reference 23, the mechanism is not described therein.

Description of Screw-Driven Traversing Probe System

General description. - Linear motion for translating the screw-driven traversing probe normal to the surface was provided by a finely threaded screw drive. The threaded shaft was driven through a gear box by an electric motor. The mast, which supported the pitot probe, was fastened to a threaded drive block. Thus, the drive block, mast, and probe were translated as the threaded shaft was rotated.

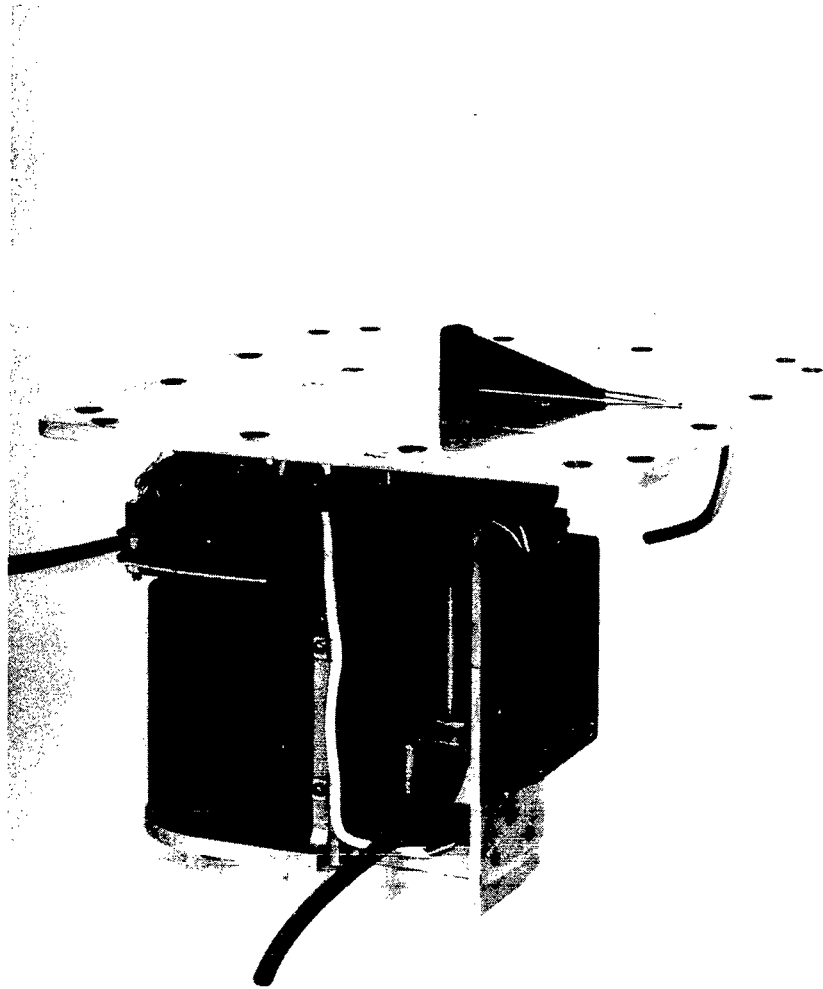
Probe height was measured by a counter which recorded the number of revolutions of the screw drive after the drive block electrically recorded its arrival at a precisely located reference point. Photographs of the single-probe version are shown in figures 4(a) and 4(b). The space required for this device beneath the surface was approximately 14.9 centimeters (5.9 inches), for depth, by 6.4 centimeters (2.5 inches) by 13.7 centimeters (5.4 inches). The weight was about 2.20 kilograms (4.85 pounds).



(a) Left side view (probe in intermediate position).

E-17352

Figure 4. Screw-driven traversing probe. F-104 flight-test-fixture installation; depth beneath skin = 14.9 cm (5.9 in.).



(b) Right side view (probe touching skin).
Figure 4. Concluded.

E-17356

The maximum travel of this prototype traversing device was about half the internal depth, the major dimension of the device. A schematic drawing of this traversing probe mechanism is shown in figure 5 together with a tabulation of the function of most of the parts. In addition, figure 5 shows the electrical circuitry, in conceptual form, which provides for driving and reversing the drive motor, recording the number of shaft revolutions, and indicating the direction of probe motion.

If the maximum travel of this probe had not been needed, a shorter traverse could have been obtained by interrupting the flow of current from the contact wiper (item ⑪, fig. 5) to a contact rail (item ⑨). A piece of tape or a spot of nonconductive cement on the rail was sufficient to stop and reverse the motor at a selected point below maximum travel. A precision adjustable reversing contact was provided at the bottom of the probe travel to insure that the probe stopped just at the skin surface (item ②, fig. 5).

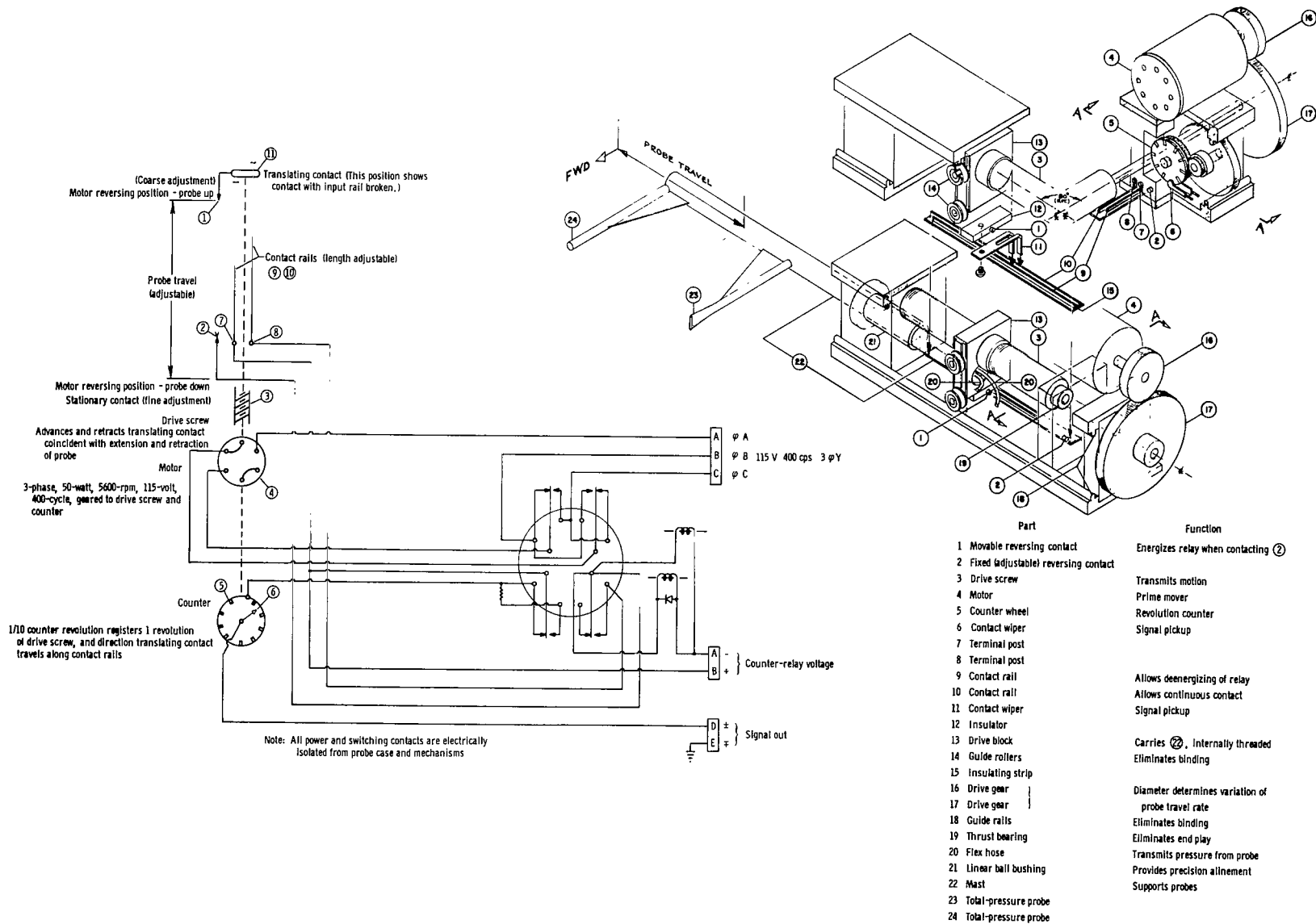


Figure 5. Electromechanical schematic of screw-driven traversing probe.

Recording methods. - For the F-104 installation, sensor outputs of shaft rotation, probe motion, direction of probe motion, and the total- and static-pressure transducers were telemetered (FM-FM) to a ground receiver and recorded on tape. These data were subsequently translated into engineering units and appropriate adjustments applied to account for shifts of the tare values from the master calibrations. An analog strip record of some of the parameters is shown in figure 6. The trace of the traversing probe total pressure is in effect a reclining profile of total pressure within the boundary layer because time, the abscissa, is related to height above the surface. Rake total pressures from a few of the fixed probes were measured on a commutating type of valve-sensor. The output of the valve-sensor is included on this analog record.

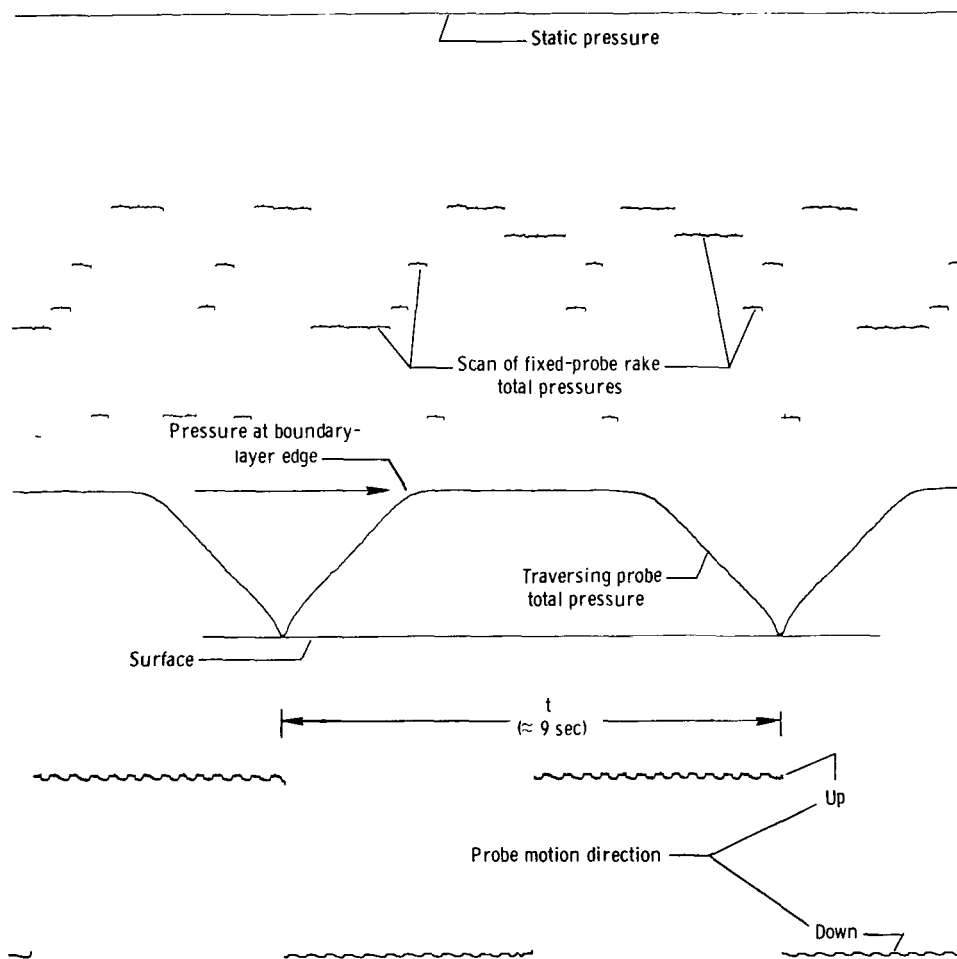


Figure 6. Analog readout of some of the parameters from the F-104 flight-test-fixture installation.

For the A5A installation the pressures were recorded on a NACA 12-cell photo-recording manometer, and the probe position count, motion direction, and stagnation temperature were recorded on an oscillograph. All data for this installation were recorded onboard the airplane and synchronized by a timer.

Operating problems. - Problems encountered during the development and demonstration of the screw-driven devices, together with the methods used to alleviate some of the problems, are discussed in the following sections.

Drive motor: Two different motors were used during the flight demonstrations. The first, on the A5A airplane, was a single-phase, 400-cycle, 115-volt motor which used approximately 20 watts to drive the probe at 1.5 to 1.8 millimeters per second (0.06 to 0.07 inch per second) when airloads were relatively low. For airloads imposed by dynamic pressures greater than approximately 14,400 N/m² (300 lb/ft²), the rate of travel was slowed, and dynamic pressures greater than 28,700 N/m² (600 lb/ft²) always stalled the device.

A larger three-phase, 400-cycle, 115-volt motor of about 50 watts was later installed on the F-104 flight-test fixture. This motor, which was geared to move the probe at about 5 millimeters per second (0.2 inch per second), operated well for dynamic pressures somewhat greater than 43,100 N/m² (900 lb/ft²), the highest attempted with this motor.

Lead of threaded drive shaft: During the first tests with the 20-watt motor installed, a fine single thread was used. It was found that the fine thread could not tolerate much wear because the threaded drive block was made of brass and there was a tendency for the brass threads to strip. Thus, after several flights, a new drive screw and block with a coarser single thread was installed which was not as susceptible to wear. The approximate lead of each thread used was:

Flight series	Installation	Lead		Thread count	
		mm	in.	per mm	per in.
First	A5A	0.176	0.00694	5.67	144
Second	F-104 flight-test fixture	.400	.01575	2.50	63.5

Precision reference position: The preceding description of the probe operation explained how the counter defined probe position relative to a precisely located reference point. Although the counter system was adequate for the prototypes described, it is believed that the position recording technique was the least satisfactory part of the probe system (i. e., the part which would profit most from further development) for the following reasons:

(1) At aerodynamic or thermal loading conditions, or both, in which thin skin would buckle, the present system might give an erroneous height value because the probe was preset¹ to reverse (at the bottom of the boundary layer) when the probe tip

¹The method of presetting, i.e., establishing a reference point, consisted of repeatedly passing a 0.075-millimeter (0.003-inch-) thick strip of paper between the probe tip and the surface while surface contact was being made. The amount of resistance the probe tip imposed on the paper strip during observations made under optimum visual conditions was evaluated. This procedure later permitted rapid final adjustments prior to flight under lighting conditions which were not optimum.

touched the surface for room temperature conditions. If buckling caused a surface dip or valley at the probe tip, it is conceivable that the probe could reverse direction without having touched the surface and without the experimenter being aware of this erroneous condition. Thus, it would be desirable to devise a probe reversal system that would be responsive to the probe touching the surface at any flight skin temperature conditions. For the screw-driven demonstrations described, the test surface was a thick plate and the temperatures were low enough that buckling did not occur.

(2) Interpreting the output signals of the counter system used for these flight demonstrations was tedious and time consuming. Therefore, it may be desirable to modify the counter system so that the output is either digitized or automatically plotted.

Boundary-Layer Profiles

The preceding sections and accompanying figures indicated that conventional boundary-layer rakes were located near the traversing probe. Figure 7 compares the

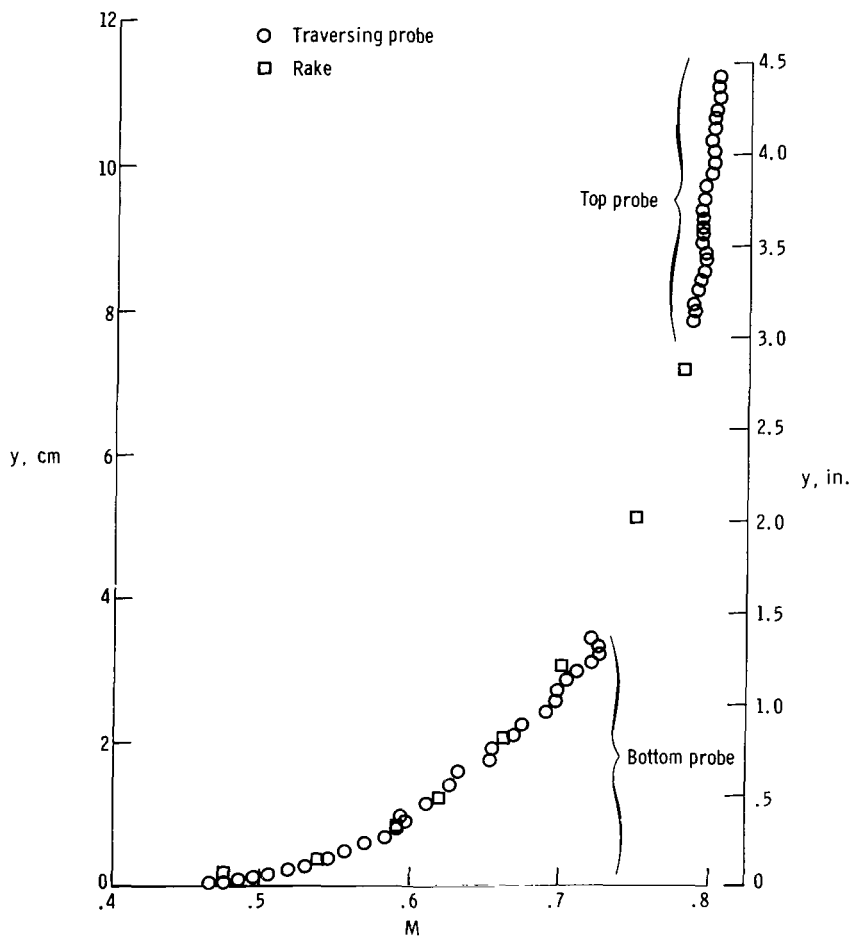
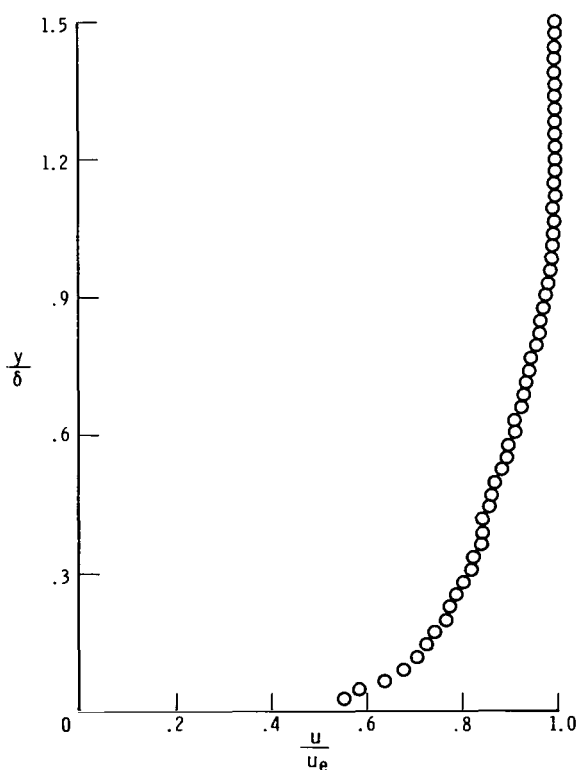


Figure 7. Mach number profile obtained with tandem traversing probe and rake. A5A installation; traverse direction upward; $M_e = 0.80$; traverse rate ≈ 0.16 cm/sec (0.06 in./sec); time for this traverse ≈ 21.6 sec.

rake and the tandem traversing probe of the A5A installation on the basis of local Mach number¹ as a function of distance from the skin. For this profile the probe was adjusted to utilize only a part of its potential traverse distance. The traversing probe results are close to the check rake values, and, of course, the traversing probe senses the boundary layer in much greater detail.

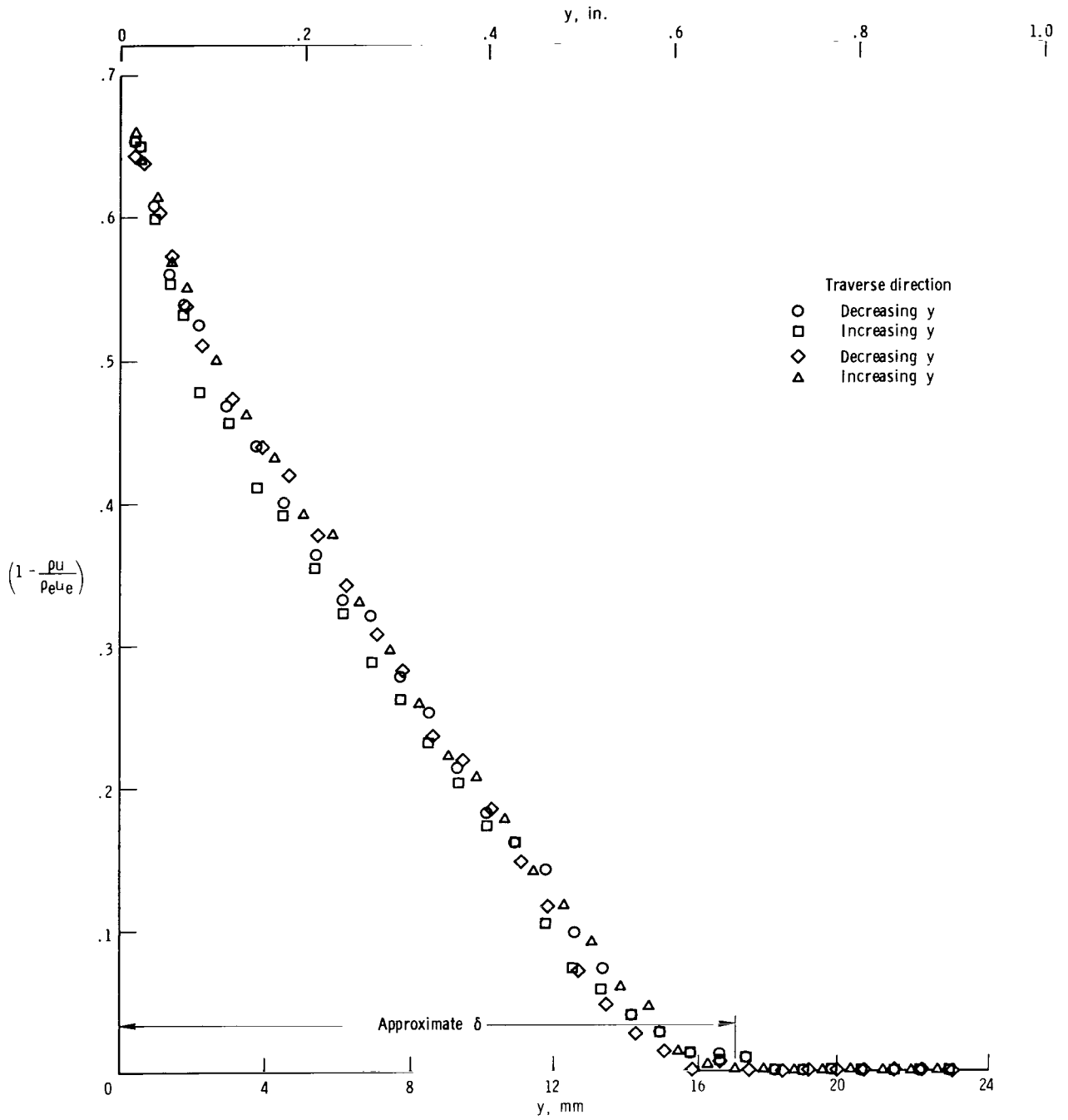
A more conventional form of boundary-layer profile presentation obtained from the F-104 flight-test-fixture installation is shown in figure 8(a). This is a single traverse obtained at an edge Mach number of 2.2. Figures 8(b) and 8(c) show the same traverse as shown in figure 8(a) and three additional traverses, obtained during the same data run, presented in terms of the displacement and momentum distributions, respectively. The methods used to compute these parameters from the traversing probe data are the same as were used in reference 23. The aircraft velocity, attitude, and altitude were held as nearly constant as possible by the pilot for 2 1/2 to 3 minutes. Comparison of the symbols indicating upward and downward movement of the probe (figs. 8(b) and 8(c)) indicates that pressure lag effects are negligible, i. e., they do not produce detectable systematic biasing of these functions at small values of y where the pressure gradient is greatest. It is therefore believed that much of the difference between the various profiles (traverses) is caused by real changes in the boundary layer resulting from small unavoidable changes in the flight conditions; changes in angle of attack and side-slip are probably the most important.



(a) Conventional velocity ratio profile; single traverse.

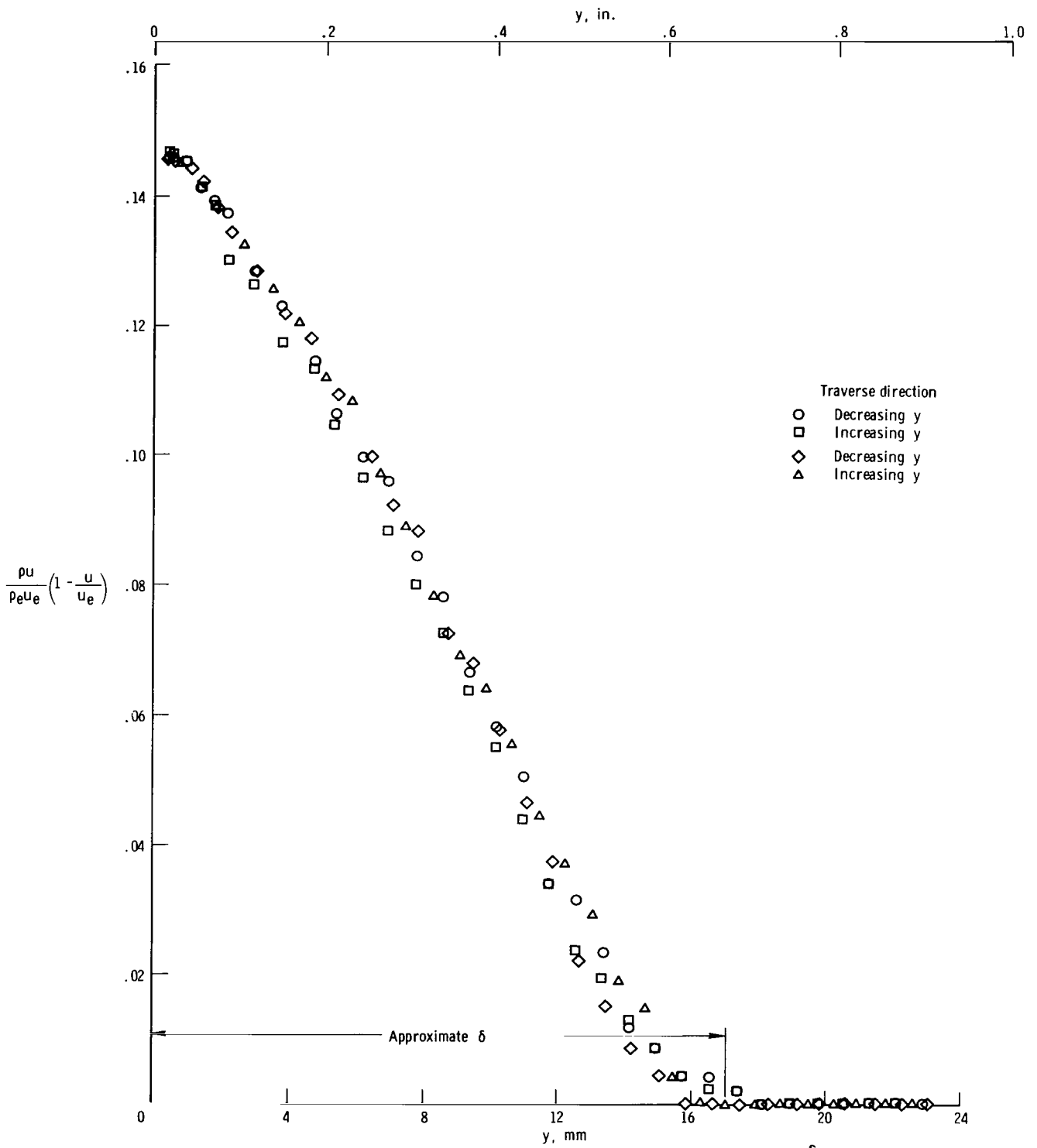
Figure 8. Boundary-layer profiles obtained with the screw-driven type of traversing probe. F-104 flight-test-fixture installation; $M_e = 2.2$; $R_x = 1.04 \times 10^7$; traverse rate ≈ 0.51 cm/sec (0.20 in./sec); time for single traverse ≈ 4.5 sec.

¹Local Mach number is derived from the relationship of local total pressure and surface static pressure in accordance with reference 24.



(b) Profile for determination of displacement thickness, δ^* ; four traverses; $\delta^* = \int_0^{\delta} (1 - \frac{\rho u}{\rho_e u_e}) dy$.

Figure 8. Continued.



(c) Profile for determination of momentum thickness, θ ; four traverses; $\theta = \int_0^{\delta} \frac{\rho u}{\rho_e u_e} \left(1 - \frac{u}{u_e}\right) dy$.

Figure 8. Concluded.

Data obtained during the traverse of figure 8(a) are presented in law-of-the-wall form in figure 9 to illustrate the usefulness of the traversing probe for defining in flight this fundamental relationship. This presentation and those of figure 8 are believed to demonstrate that this traversing mechanism and sensor combination is adequate for surveying a turbulent boundary layer, although a more precise pressure sensor (transducer) is advisable for a deliberate study of boundary-layer characteristics. The range of the transducer used was not optimum for this task, as suggested by the relative displacement of two data points near the bottom of the profile.

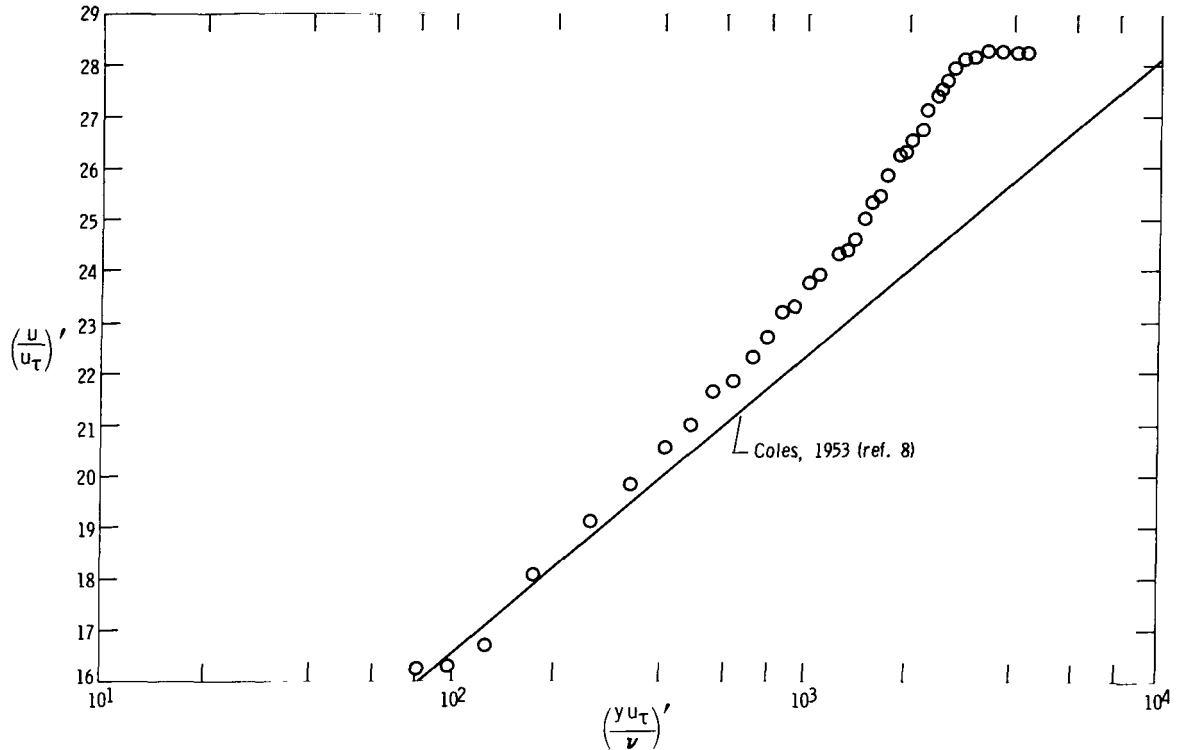


Figure 9. Example of law-of-the-wall presentation of flight data transformed to incompressible conditions by the method of reference 22 from edge condition of $M_e = 2.2$. F-104 flight-test-fixture installation; $R_x = 1.04 \times 10^7$.

A natural and useful combination of the law-of-the-wall type of presentation and the traversing probe is the Clauser type of local friction determination (ref. 25). Reference 26 provides a convenient means of using the Clauser determination of local friction through charts derived from the friction law of Fenter and Stalmach (ref. 10). An example of a profile obtained with the traversing probe and applied to the charts of reference 26 is shown in figure 10. The flight data represent the same traverse as shown in figures 8(a) and 9. The local value of friction coefficient interpolated from this profile is 0.00162 to 0.00165, neglecting the two data points which correspond to the low values discussed in connection with figure 9. The presentations of figures 9 and 10 for the wall law and the Clauser determination require closely spaced readings. The traversing probe provided the required density of data. In view of the spacing of data points shown for these profiles (for most of the profile the spacing was 0.400 mm (0.01575 in.)), it can be seen that a conventional rake would have provided a sparse profile at best compared to the results from the screw-driven probe in figures 7 to 10.

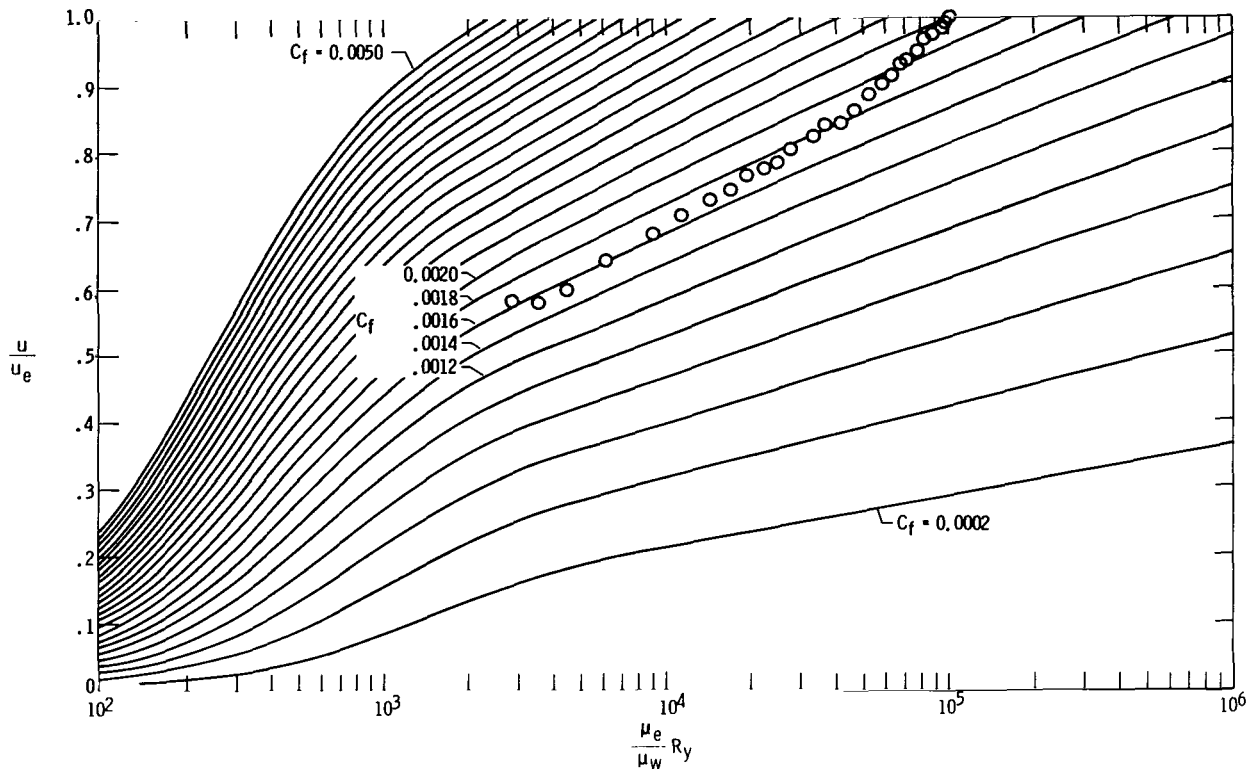


Figure 10. Example of traversing probe data from F-104 flight-test-fixture installation presented with curves from reference 26 for interpolation of local skin-friction coefficients at $M_e = 2.20$.

Several profiles obtained from traversing probes installed on both the F-104 flight-test fixture and the A5A airplane were interpreted in terms of local skin-friction coefficient, C_f , through the charts of reference 26. These profiles are presented as C_f versus momentum thickness Reynolds number, transformed to incompressible conditions, in figure 11. The flight values represent 15 traverses taken from 12 discrete flight conditions. The flow is considered quasi-two-dimensional, in that the surface of the flight-test fixture was flat and the underside of the A5A airplane provided a ratio of boundary-layer thickness to local surface radius of curvature between 2 percent and 4 percent.

The relationship of the flight data to the flat-plate incompressible curve of Kármán-Schoenherr (ref. 27) is believed to demonstrate that the traversing probe is an acceptable in-flight boundary-layer survey device. The scatter in the flight data is not considered to be excessive, in that the sensor ranges for these demonstrations were not optimized. Furthermore, the slope of local friction with Reynolds number for the flight data and the Kármán-Schoenherr curve are in excellent agreement.

It is believed that the screw-driven traversing probe concept has been successfully demonstrated as a means for deriving quasi-steady-state boundary-layer profile data in flight. Thus, as has already occurred in wind tunnels, it is expected that further development and refinement will make this concept a versatile flight-research tool. The most probable avenues for further development are expected to lead to: (1) an

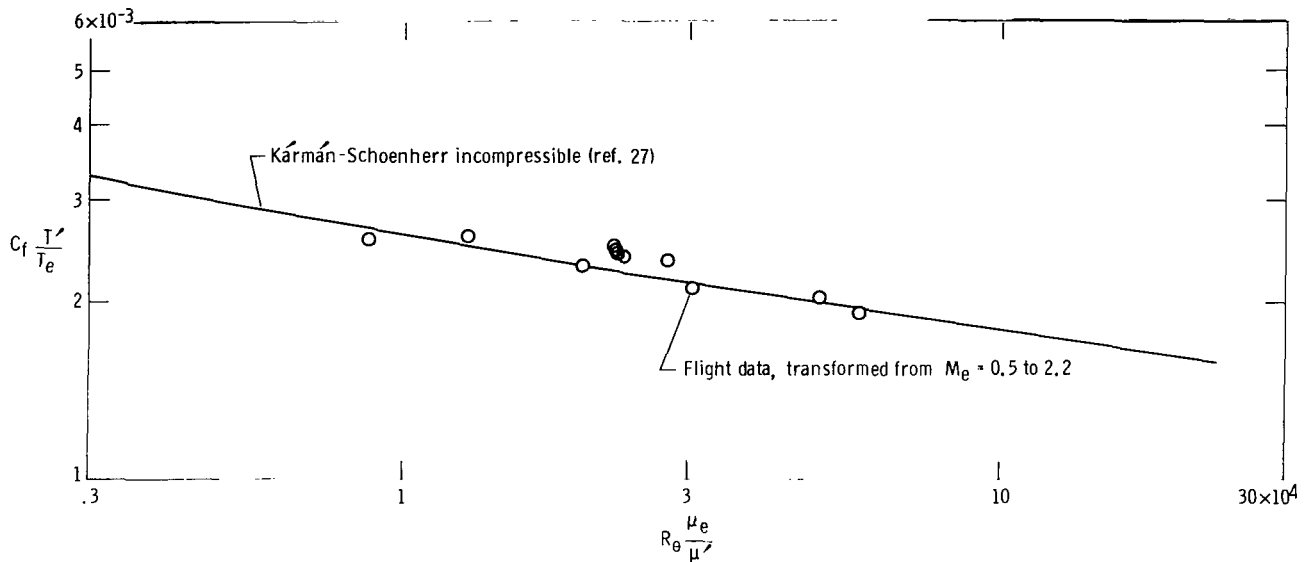


Figure 11. Comparison of local friction coefficients derived from traversing probe data and the charts of reference 26 with the Kármán-Schoenherr relationship for a flat plate.

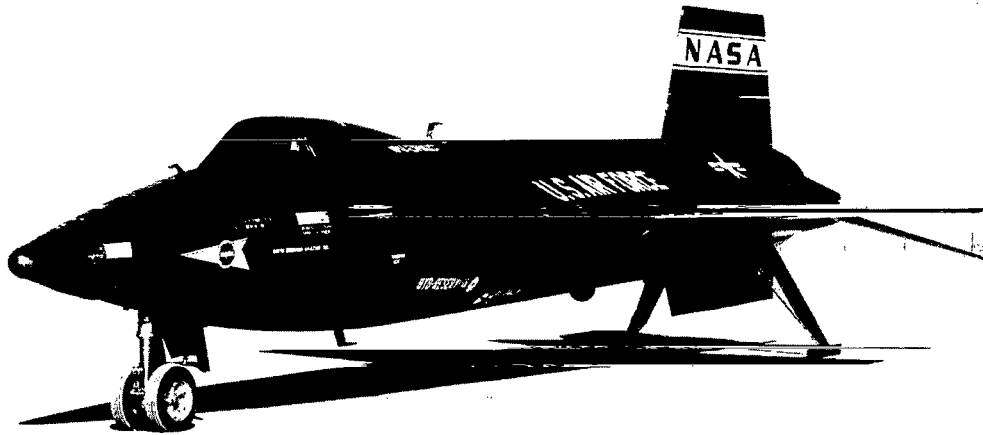
improved position recording technique, (2) a more compact, lighter weight design with a proportionally larger traverse distance, (3) the capability of measuring local flow angle simultaneously with position and local total pressure, (4) the capability of measuring high-frequency velocity components, and (5) the extension of the traversing concept in flight to other fluid flow parameters such as local static pressure or total temperature.

SCOTCH-YOKE-DRIVEN TRAVERSING PROBE

Airplane Used and Test Conditions

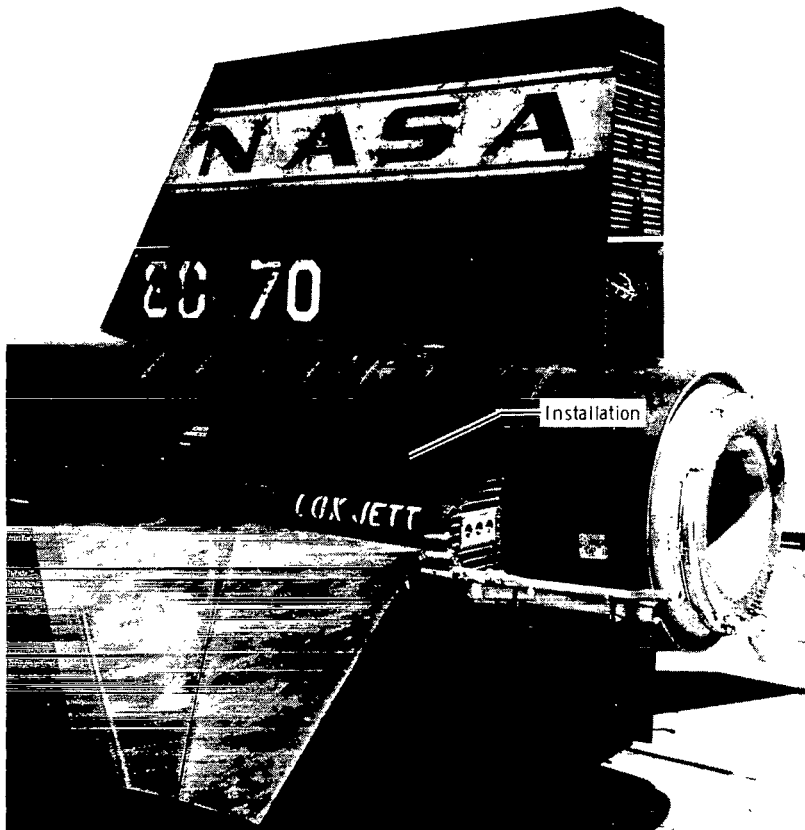
A traversing probe driven by a Scotch yoke mechanism was installed on an X-15 airplane. The airplane provided test velocities up to a free-stream Mach number of 5.6 and altitudes in excess of 30.5 kilometers (1×10^5 feet). Information about the major X-15 research objectives and operational procedures is presented in reference 28. The X-15 airplane, a rocket-powered vehicle with a thrust-to-weight ratio between 2 to 4, produced rapidly changing flow conditions. Thus it provided the variable flow conditions and somewhat elevated temperatures which may be necessary to evaluate the traversing probe concept for possible future research aircraft which accelerate rapidly to hypersonic speeds. The Scotch yoke type of drive was chosen as an easier way to achieve traverse speeds which were faster than those of the screw-driven probes and which could accommodate the rapid aircraft acceleration.

A photograph of the X-15 airplane is shown in figure 12(a). The traversing probe was installed on the upper surface of the left side fairing adjacent to the vertical- and horizontal-tail surfaces. Figure 12(b) shows a closeup view of the probe installation and the adjacent tail surfaces.



(a) Three-quarter front view.

E-7902



(b) View of region in which Scotch-yoke-driven traversing probe was installed.
Figure 12. X-15 airplane used to demonstrate Scotch-yoke-driven traversing probe.

External Installation Details

The traversing probe was installed in the side fairing region to provide quasi-two-dimensional flow adjacent to internal aircraft volume sufficient to contain the traversing mechanism and the pressure recorder. However, even though the surface immediately surrounding the probe and upstream of it was relatively flat, the local flow approached two-dimensional conditions only intermittently. This was caused by continually changing interference from adjacent tail surfaces, the speed brakes, and occasional upstream venting of the liquid oxygen tank as free-stream Mach number, altitude, and angle of attack varied.

The length of the turbulent run upstream of the installation was known from previous studies to be about 14.2 meters (46.6 feet). This generated a boundary layer estimated to be 18 to 20 centimeters (7 to 8 inches) thick. The total traverse distance of this probe device was about 5.1 centimeters (2.0 inches), so only the bottom, high gradient, portion of the boundary layer was sampled. This was necessitated by a space limitation at the installation location. Thus the highest Mach number actually sampled by the probe was about 2.2, even though the free-stream Mach number was above 5.

The probe is shown fully extended in figure 13 along with an accompanying two-probe check rake and two flush static orifices. The panel upon which these devices were mounted was almost flat, but, as the juncture with the fuselage indicates, the inboard region was slightly curved.

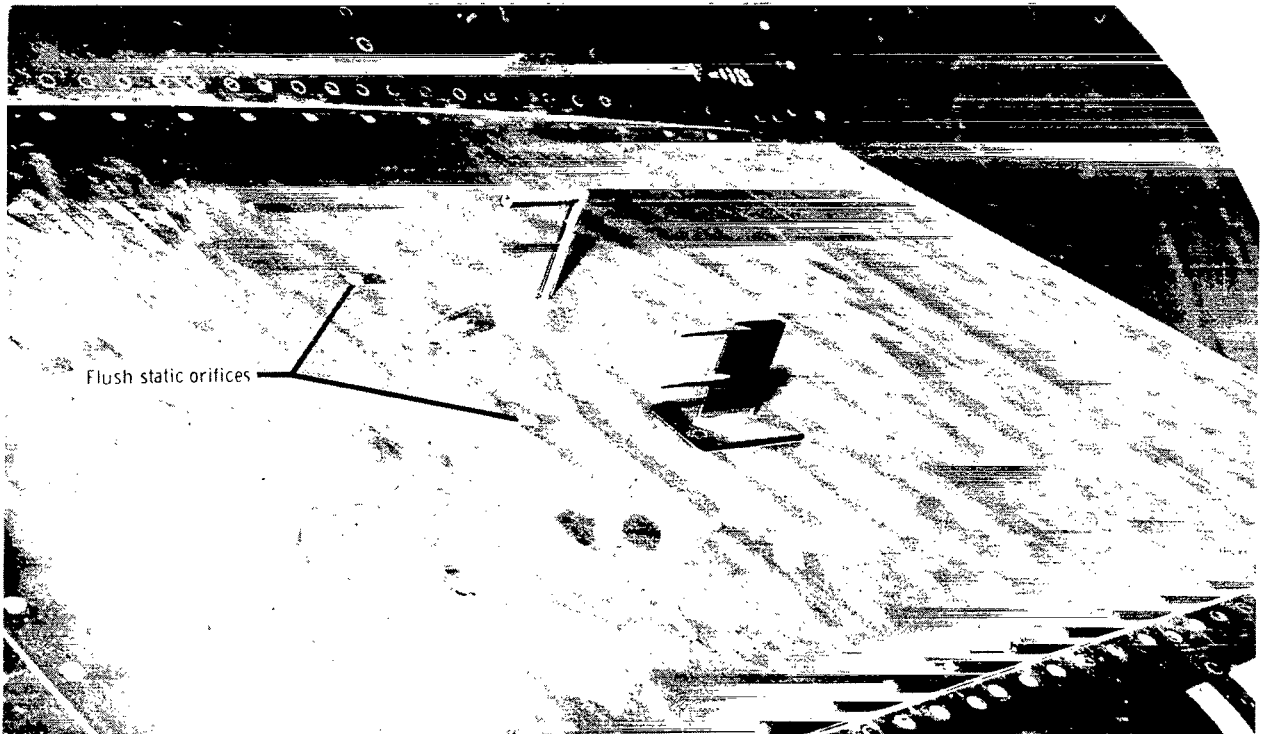


Figure 13. Closeup of Scotch-yoke-driven traversing probe installation.

E-9913

The sensing manometer for this installation was placed just beneath the skin and immediately aft of the probe station, so the pressure lines were short enough to insure negligible lag.

Description of Traversing Probe

General description.— The Scotch yoke drive used for this installation had a faster traverse rate--15 cycles a minute--than that of the screw-driven probes.

The approximate physical dimensions of this device were as follows:

Depth including linear potentiometer, cm (in.)	27.9 (11.0)
Depth without linear potentiometer, cm (in.)	15.2 (6.0)
Dimension parallel with crank axis, cm (in.)	8.9 (3.5)
Dimension parallel with yoke slot, cm (in.)	10.8 (4.3)
Traverse distance, cm (in.)	5.1 (2.0)
Weight including motor and potentiometer, kg (lb)	1.44 (3.17)

Because the action of the Scotch yoke was somewhat like that of the crank shaft and piston action in a reciprocating engine, the position-time relationship at the top and bottom of the cycle was consistently smooth. (The position-time relationship is a sine wave.) A screw-drive mechanism which would have a large lead and a corresponding high traverse rate would not only have been harder to decelerate and reverse at the ends of the stroke but extensive drive block wear would probably have occurred.

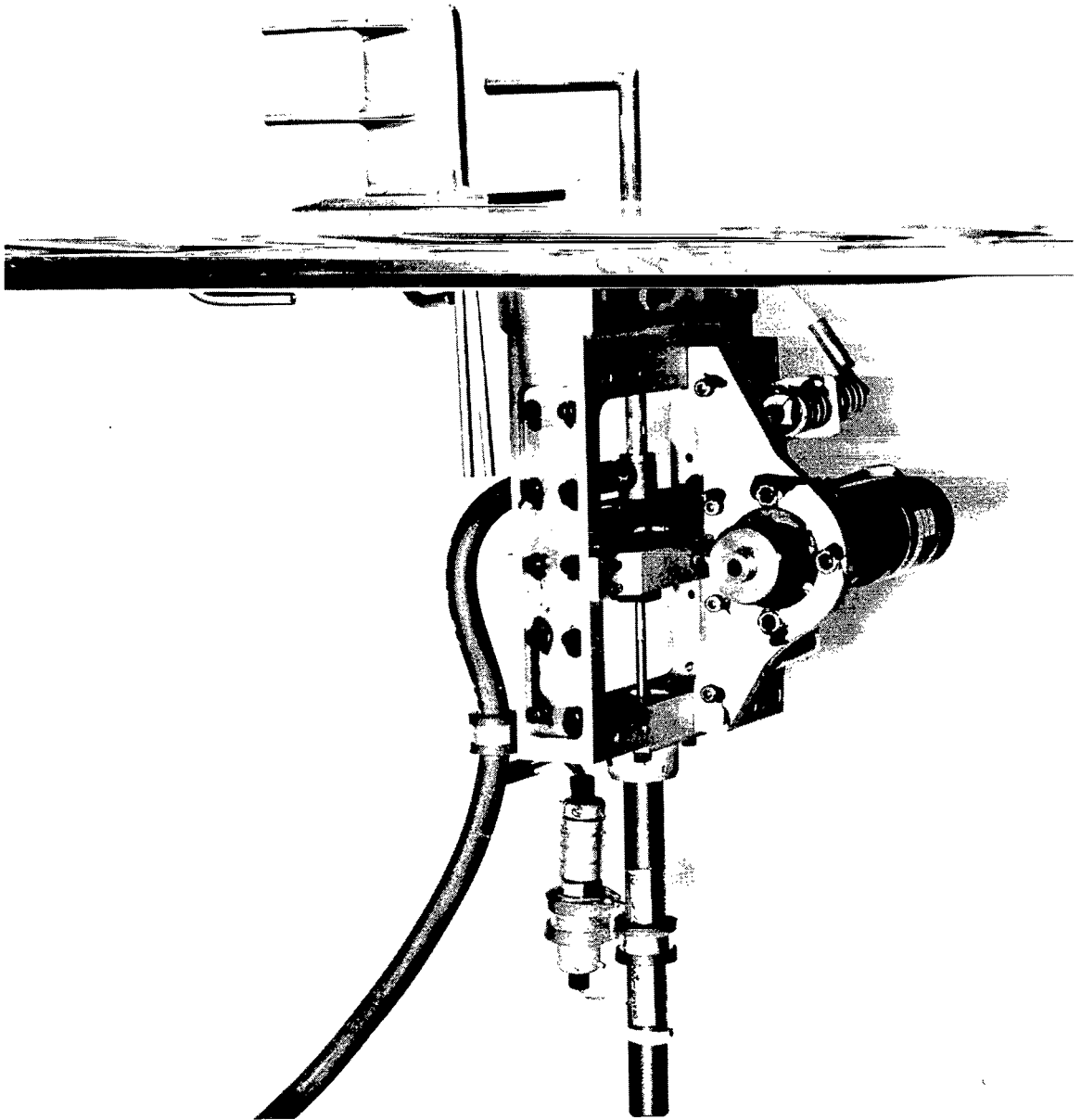
The means by which a traversing motion was achieved is shown in the photographs of figure 14 and the drawing of figure 15. The drive train, consisting of bevel gears and the crank mechanism, was conventional; however, the method of obtaining a smooth action may be worthy of discussion.

The use of ball-bearing rollers (item ②⑥, fig. 15) at the ends of the yoke carrier (item ②①) helped eliminate sliding friction with a minimum of binding. In addition, item ⑨ of the crank arm is a ball bearing which rolled in the carrier slot (item ②②), and the mast of the probe (item ①) traversed through a linear ball bushing (item ②⑤). Each of these ball bearings or bushings was important as a means of eliminating sliding friction and insuring a smooth traverse.

Probe position was sensed by a rectilinear potentiometer, and the output was recorded on an oscillograph. The pressures from the traversing probe, check rake, and static orifices were recorded on an NACA type of 12-cell photorecording manometer. These records were synchronized by a timer.

Operating problems.— Problems encountered during the development and demonstration of this device, and solutions, where available, are discussed in the following sections.

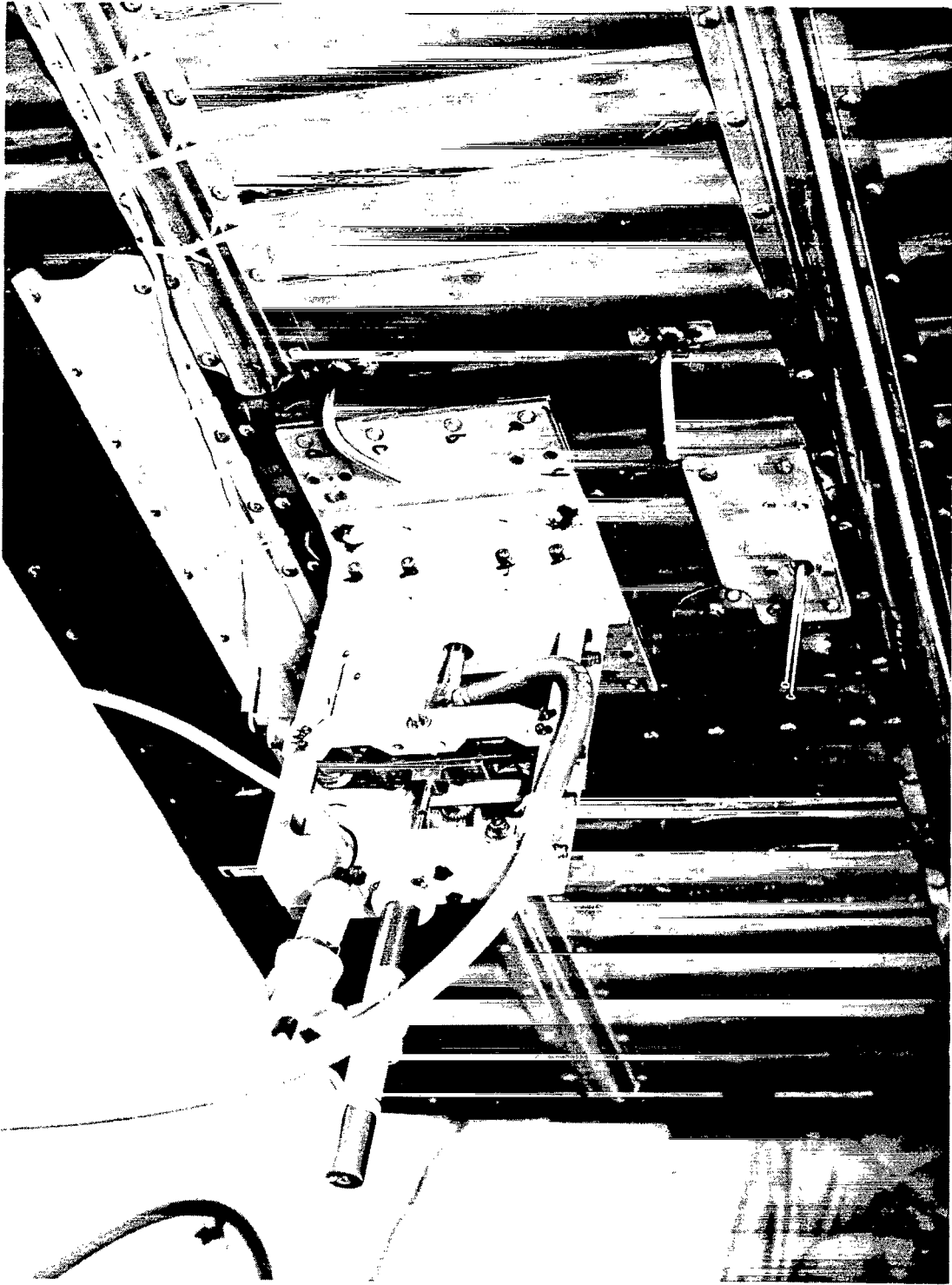
Drive motor: The motor used for this installation was the same motor described as inadequate for the A5A installation of the screw-driven probe. On the Scotch yoke traversing probe, the performance of the motor was marginal. The 50-watt, three-phase motor mentioned previously would also have been better for the Scotch yoke mechanism than the motor used.



(a) Side view.

E-9909

Figure 14. Scotch-yoke-driven traversing probe (mechanism in mid traverse). Height of fixed rake = 5.1 cm (2.0 in.).



(b) Front view.

E-9911

Figure 14. Concluded.

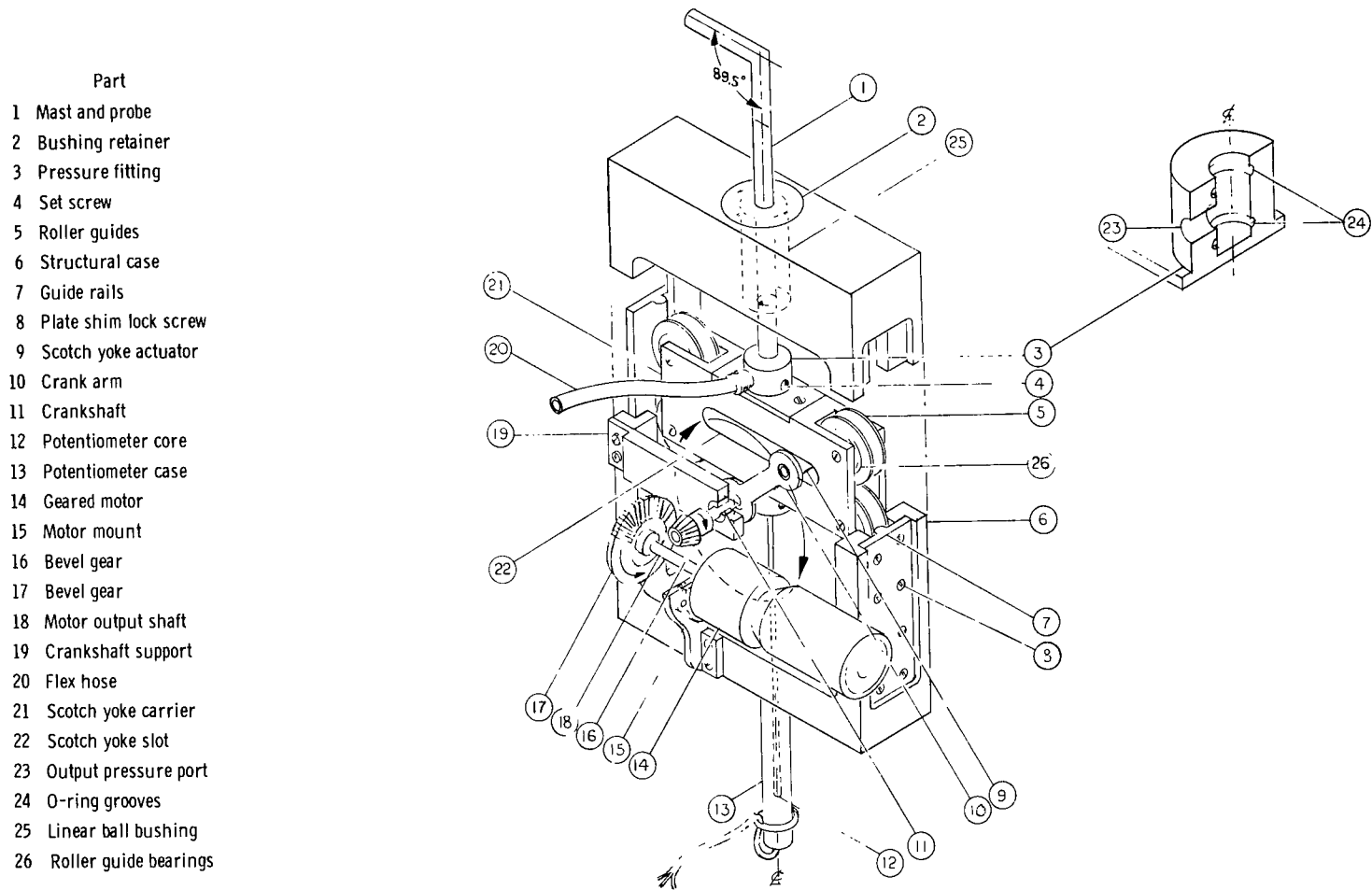


Figure 15. Drawing of Scotch-yoke-driven traversing probe.

Rough traverse action: Ball bearings and bushings (previously mentioned) were used to overcome sliding friction after an early bench model proved to have a rough chattering action despite careful machining and precise alinement of the moving parts. Elimination of sliding friction through the use of the ball bearings provided a smooth action. This was achieved before the traversing probe was installed on the airplane.

Aerodynamic heating of the skin: The smooth action obtained during ground runs, after the sources of sliding friction were eliminated, was interrupted during the first flight. Aerodynamic heating of the skin to about 610° K (1100° R) caused the mast of the traversing probe to bind against the skin as it moved within the hole in the skin. The binding was severe enough that the motor stopped because the drive motor fuse overheated. After the flight, the region of contact which caused the binding was easily detected and the hole was slightly enlarged, thus eliminating this source of trouble.

Flow uniformity: During much of a flight the flow quality was not good enough to permit the device to be evaluated. Shocks from adjacent protuberances interfered with comparisons between the traversing probe and the two-probe check rake. At some supersonic speeds the traversing probe interfered with the flow past the adjacent rake because of crossflow effects, and, after the aircraft rocket engine was shut down, intermittent venting of the liquid oxygen tank of the propulsion system caused erratic flow over the test region. These problems of flow uniformity were not a reflection on the integrity of the traversing probe, but they did interfere with an orderly evaluation and limited the quantity of useful data.

Results From the Scotch-Yoke-Driven Traversing Probe

As indicated in the previous section, comparison of traversing probe data with the two-probe check rake results was restricted over a large portion of a flight because of poor (nonuniform) flow quality. Profile data could be obtained over much of a flight, but comparisons with the check rake were meaningful only during captive flight at subsonic speeds when the X-15 airplane was still attached to the launch airplane.

A sample of such a comparison is shown in figure 16. Total pressures obtained from the traversing probe and the rake probes are compared over a period involving about 3 1/2 cycles. These data are for those points in time when the traversing probe position is equal to either of the fixed-probe heights above the skin. Also shown is the percentage deviation of the traversing probe values from the fixed-rake values for each of these instances. When more experience from three flights is considered (over 100 samples), the standard deviation of total-pressure differences between the traversing probe and the fixed probes is 1.2 percent. The predicted absolute standard deviation of total-pressure error based upon the physical characteristics of the sensors was 1.1 percent, assuming that the errors in determining probe position were negligible. Thus it appears that the effects of position uncertainty and pressure lag induced by the boundary-layer profile gradient are virtually negligible for steady flight conditions.

Data obtained at high supersonic speeds are presented in figure 17. The data are presented as the ratio of the unsmoothed local total pressure to local surface static pressure and the probe height, each as a function of time. The free-stream Mach number for these data was 5.6, corresponding to stagnation temperatures of about 1675° K (3020° R). The relationship of the pressure profile to the position profile

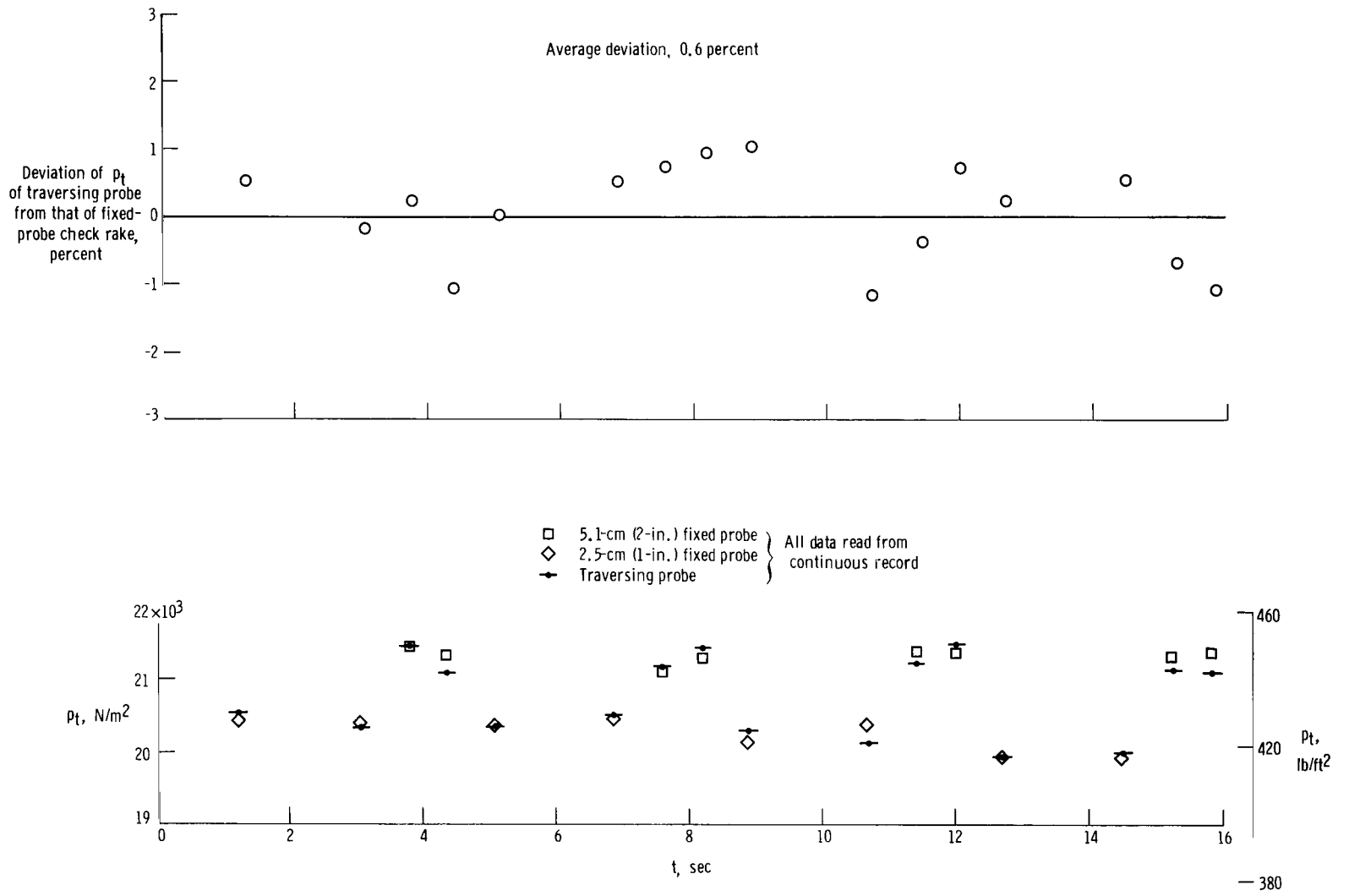


Figure 16. Comparison of traversing probe results, for about 3 1/2 cycles, with adjacent fixed-probe check rake results for a free-stream Mach number of approximately 0.8.

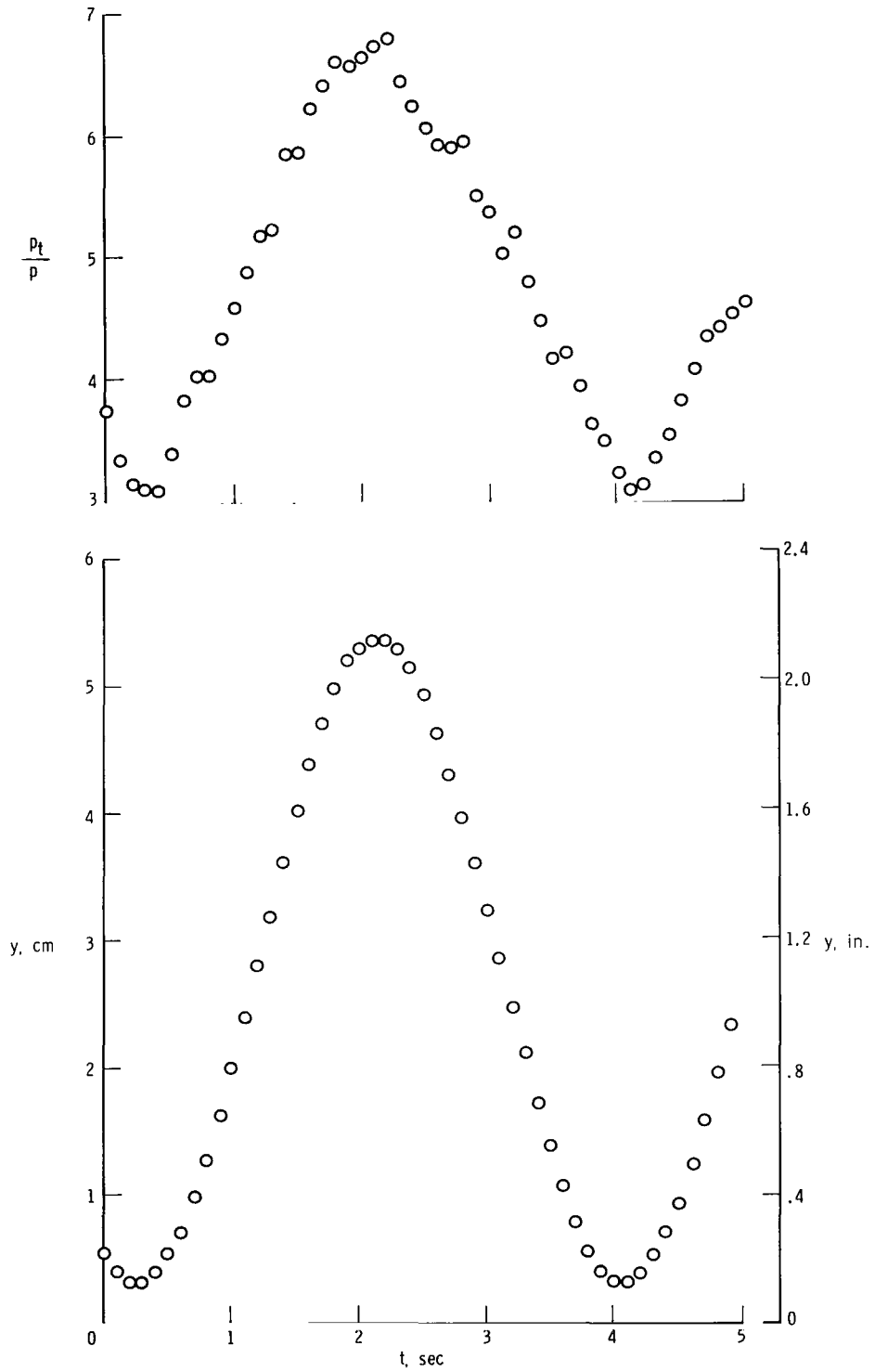


Figure 17. History of local total-to-static-pressure ratio and probe position obtained with Scotch-yoke-driven traversing probe for a free-stream Mach number of 5.6.

indicates that the response of the system was adequate to describe the high gradient portion of this boundary layer when the probe was traversing at the rate of 15 cycles per minute. The data of figures 16 and 17 indicate that the Scotch-yoke-driven traversing probe can provide useful boundary layer, or inviscid shear layer, data for traverses through pressure gradients at relatively high traverse rates. A maximum gradient of pressure which can be reliably recorded by this device cannot be quantitatively defined from the present study. Because the travel of this probe was limited to the lower, high gradient, portion of the boundary layer, it was not possible to derive local friction or boundary-layer thickness parameters. It is believed, however, that these boundary-layer parameters could be defined through the use of the Scotch-yoke-driven device if travel completely through the boundary layer was provided.

On the basis of these results and the operating experience, it is believed that the Scotch-yoke-driven device can more easily achieve high traverse rates with smooth direction changes and little wear than the screw-driven device used in this study. The screw-driven device provided the most accurate position measurements (distance from skin); however, through refinements, either type of traversing mechanism could provide closely spaced data readings and precise position values because the methods used to determine position need not depend on the type of drive mechanism.

CONCLUDING REMARKS

Two prototype traversing probes, a screw-driven and a Scotch-yoke-driven, were demonstrated in flight to supersonic speeds. The screw-driven model was shown to be a useful means of deriving local skin friction and other boundary-layer parameters for quasi-steady-state flight conditions to boundary-layer edge Mach numbers of 2.2. Of the two types of devices, the screw-driven model provided the most accurate position measurements (distance from skin).

The Scotch yoke model was exposed to much more severe conditions than the screw-driven model in that the flow conditions changed rapidly and the maximum total temperature in the boundary layer was about 1675° K (3020° R), generated by a free-stream Mach number of 5.6. This probe performed well mechanically under these conditions, and the traverse rate and response of the sensors were adequate to describe the high gradient portion of the boundary layer. It is believed that the Scotch yoke device can more easily achieve high traverse rates with smooth direction changes and little wear than the screw-driven model.

It was shown that the screw-driven type of traversing probe can provide the closely spaced readings required by the wall-law presentation and the related Clauser type of presentation. The Scotch yoke type of device should also be able to provide adequate density of data if provided with an improved position-indicating device.

Neither type of traversing probe was optimized for compactness or light weight. Thus, it is expected that design effort toward such optimization will be successful. After the mechanical design is optimized, it is expected that the traversing sensor

concept in flight will be applied to other fluid flow parameters including total-temperature and high-frequency measurements of velocity components.

Flight Research Center,
National Aeronautics and Space Administration,
Edwards, Calif., January 22, 1971.

REFERENCES

1. Samuels, Richard D. : Experimental Investigation of the Turbulent Boundary Layer on a Typical Subsonic Transport Fuselage. NASA TN D-5242, 1969.
2. Hopkins, Edward J. ; and Keener, Earl R. : Study of Surface Pitots for Measuring Turbulent Skin Friction at Supersonic Mach Numbers - Adiabatic Wall. NASA TN D-3478, 1966.
3. Cornish, Joseph J. , III; and Roberts, Sean C. : Impervious Turbulent Boundary Layer Measurements Using an Integrating Boundary Layer Mouse. Res. Note No. 17, Mississippi State Univ. , July 1963.
4. Erlich, E. : Sondage de la Couche Limite en Vol Supersonique sur L'Avion "Mirage IV. " ONERA paper presented at 3^e Colloque Aerodynamique de l'A. F. I. T. A. E. , Marseille, France, Nov. 8-10, 1966.
5. Freeman, Hugh B. : Measurements of Flow in the Boundary Layer of a 1/40-Scale Model of the U. S. Airship "Akron. " NACA Rept. No. 430, 1932.
6. Dryden, Hugh L. : Air Flow in the Boundary Layer Near a Plate. NACA Rept. No. 562, 1936.
7. Klebanoff, P. S. ; and Diehl, Z. W. : Some Features of Artificially Thickened Fully Developed Turbulent Boundary Layers With Zero Pressure Gradient. NACA Rept. 1110, 1952.
8. Coles, Donald: Measurements in the Boundary Layer on a Smooth Flat Plate in Supersonic Flow. Jet Prop. Lab. , Calif. Inst. Technol.
I. The Problem of the Turbulent Boundary Layer. Rep. No. 20-69, June 1, 1953.
II. Instrumentation and Experimental Techniques at the Jet Propulsion Laboratory. Rep. No. 20-70, June 1, 1953.
9. Nothwang, George J. : An Evaluation of Four Experimental Methods for Measuring Mean Properties of a Supersonic Turbulent Boundary Layer. NACA Rept. 1320, 1957. (Supersedes NACA TN 3721.)
10. Fenter, Felix W. ; and Stalmach, Charles J. , Jr. : The Measurement of Local Turbulent Skin Friction at Supersonic Speeds by Means of Surface Impact Pressure Probes. DRL 392, Univ. of Texas, Oct. 21, 1957.
11. Smith, Donald W. ; and Walker, John H. : Skin-Friction Measurements in Incompressible Flow. NASA TR R-26, 1959. (Supersedes NACA TN 4231.)
12. Matting, Fred W. ; Chapman, Dean R. ; Nyholm, Jack R. ; and Thomas, Andrew G. : Turbulent Skin Friction at High Mach Numbers and Reynolds Numbers in Air and Helium. NASA TR R-82, 1961.

13. Roensch, R. L. : Investigation of Skin Friction Drag on Practical Construction Surfaces for the SST. Rept. No. 31239, Douglas Aircraft Company, Inc. , Apr. 1, 1963.
14. Jackson, Mary W. ; Czarnecki, K. R. ; and Monta, William J. : Turbulent Skin Friction at High Reynolds Numbers and Low Supersonic Velocities. NASA TN D-2687, 1965.
15. Allen, Jerry M. ; and Monta, William J. : Turbulent-Boundary-Layer Characteristics of Pointed Slender Bodies of Revolution at Supersonic Speeds. NASA TN D-4193, 1967.
16. Laverré, Jean: Pitot Boundary Layer Probes With Position Indicators Using Extensometric Gauges. ONERA paper presented at the 32nd Supersonic Tunnel Association Meeting, Stockholm, Sept. 18-19, 1969.
17. Weidinger, Hamns: Drag Measurements on a Junkers Wing Section. NACA TM No. 428, 1927.
18. Bicknell, Joseph: Determination of the Profile Drag of an Airplane Wing in Flight at High Reynolds Numbers. NACA Rept. No. 667, 1939.
19. Roberts, Sean C. : A Flight Investigation of Profile Drag Measurements. Res. Note No. 16, Mississippi State Univ. , Dec. 15, 1962.
20. Anon. : Heat Transfer and Fluid Flow - A Compilation. NASA SP-5920(01), 1968.
21. Mechtly, E. A. : The International System of Units - Physical Constants and Conversion Factors. NASA SP-7012, 1969.
22. Sommer, Simon C. ; and Short, Barbara J. : Free-Flight Measurements of Turbulent-Boundary-Layer Skin Friction in the Presence of Severe Aerodynamic Heating at Mach Numbers From 2.8 to 7.0. NACA TN 3391, 1955.
23. Saltzman, Edwin J. ; and Fisher, David F. : Some Turbulent Boundary-Layer Measurements Obtained From the Forebody of an Airplane at Mach Numbers up to 1.7. NASA TN D-5838, 1970.
24. Ames Research Staff: Equations, Tables, and Charts for Compressible Flow. NACA Rept. 1135, 1953. (Supersedes NACA TN 1428.)
25. Clauser, Francis H. : Turbulent Boundary Layers in Adverse Pressure Gradients. J. Aeron. Sci. , vol. 21, no. 2, 1954, pp. 91-108.
26. Allen, Jerry M. ; and Tudor, Dorothy H. : Charts for the Interpolation of Local Skin Friction From Experimental Turbulent Velocity Profiles. NASA SP-3048, 1969.
27. Peterson, John B. , Jr. : A Comparison of Experimental and Theoretical Results for the Compressible Turbulent-Boundary-Layer Skin Friction With Zero Pressure Gradient. NASA TN D-1795, 1963.

28. Weil, Joseph: Review of the X-15 Program. NASA TN D-1278, 1962.

NATIONAL AERONAUTICS AND SPACE ADMINISTRATION

WASHINGTON, D. C. 20546

OFFICIAL BUSINESS

PENALTY FOR PRIVATE USE \$300

FIRST CLASS MAIL



POSTAGE AND FEES PAID
NATIONAL AERONAUTICS AND
SPACE ADMINISTRATION

06U 001 26 51 3DS 71166 00903
AIR FORCE WEAPONS LABORATORY /WL0L/
KIRTLAND AFB, NEW MEXICO 87117

ATT E. LOU BOWMAN, CHIEF, TECH. LIBRARY

POSTMASTER: If Undeliverable (Section 158
Postal Manual) Do Not Return

"The aeronautical and space activities of the United States shall be conducted so as to contribute . . . to the expansion of human knowledge of phenomena in the atmosphere and space. The Administration shall provide for the widest practicable and appropriate dissemination of information concerning its activities and the results thereof."

— NATIONAL AERONAUTICS AND SPACE ACT OF 1958

NASA SCIENTIFIC AND TECHNICAL PUBLICATIONS

TECHNICAL REPORTS: Scientific and technical information considered important, complete, and a lasting contribution to existing knowledge.

TECHNICAL NOTES: Information less broad in scope but nevertheless of importance as a contribution to existing knowledge.

TECHNICAL MEMORANDUMS:
Information receiving limited distribution because of preliminary data, security classification, or other reasons.

CONTRACTOR REPORTS: Scientific and technical information generated under a NASA contract or grant and considered an important contribution to existing knowledge.

TECHNICAL TRANSLATIONS: Information published in a foreign language considered to merit NASA distribution in English.

SPECIAL PUBLICATIONS: Information derived from or of value to NASA activities. Publications include conference proceedings, monographs, data compilations, handbooks, sourcebooks, and special bibliographies.

TECHNOLOGY UTILIZATION PUBLICATIONS: Information on technology used by NASA that may be of particular interest in commercial and other non-aerospace applications. Publications include Tech Briefs, Technology Utilization Reports and Technology Surveys.

Details on the availability of these publications may be obtained from:

SCIENTIFIC AND TECHNICAL INFORMATION OFFICE

NATIONAL AERONAUTICS AND SPACE ADMINISTRATION

Washington, D.C. 20546